IEEE Access
Multidisciplinary | Rapid Review | Open Access Journal

Received 15 February 2023, accepted 7 April 2023, date of publication 17 April 2023, date of current version 3 May 2023.

Digital Object Identifier 10.1109/ACCESS.2023.3267963

RESEARCH ARTICLE

Reproducing Tactile and Proprioception Based on the Human-in-the-Closed-Loop Conceptual Approach

SAEED BAHRAMI MOQADAM[1], KNOLLIS DELLE[2], URSUS SCHORLING[3], AHMAD SALEH ASHEGHABADI[1], FARZANEH NOROUZI[4], AND JING XU[1], (Member, IEEE)

[1]State Key Laboratory of Tribology, Beijing Key Laboratory of Precision/Ultra-Precision Manufacturing Equipment Control, Department of Mechanical Engineering, Tsinghua University, Beijing 100084, China
[2]Department of Engineering Physics, Tsinghua University, Beijing 100084, China
[3]Mechanical Department, Leibniz University Hannover, 30167 Hannover, Germany
[4]Department of Cardiology, Mashhad University of Medical Sciences, Mashhad 13131-99137, Iran

Corresponding authors: Saeed Bahrami Moqadam (Sayd17@mails.tsinghua.edu.cn) and Jing Xu (jingxu@tsinghua.edu.cn)

This work was supported in part by the Beijing Municipal Natural Science Foundation under Grant L192001, in part by the National Natural Science Foundation of China (NSFC) under Grant 62173198 and Grant 51935010, and in part by the State Key Laboratory of Tribology of China under Grant SKL2020C15.

This work involved human subjects or animals in its research. Approval of all ethical and experimental procedures and protocols was granted by the Institution Review Board of Tsinghua University under Application No. 20210136, and performed in line with the Helsinki Declaration.

ABSTRACT Prosthetic limb embodiment remains a significant challenge for many amputees due to traditional designs' lack of sensory feedback. To address this challenge, the effectiveness of non-invasive neuromuscular electrical stimulation (NMES) controlled by a hybrid proportional-differential (PD)-Fuzzy logic system was evaluated for providing real-time proprioception and tactile feedback. The study used a human-in-the-closed-loop approach with ten participants: five upper limb amputees and five non-disabled individuals as the control group. An applied force, the joint angle of a prosthetic hand's finger, and surface electromyography signals generated by the biceps muscle all regulate the intensity of sensory feedback. Additionally, the C6 and C7 myotomes were selected as elicitation sites. The average threshold for detecting action motion and force was around 21° and 1.524N, respectively. The participants successfully reproduced desired joint angles within the range of 0°-110° at five separate intervals. In the weight recognition experiment, the amputee participant's minimum number of false predictions was four. The highest accuracy achieved was 80.66% in detecting object size and stiffness. Additionally, unpaired t-tests were performed for the means of the results of the experiments to determine statistically significant differences between groups. The results suggest that stimulation of myotomes by NMES is an effective non-invasive method for delivering rich multimodal sensation information to individuals with disabilities, including upper limb amputees, without needing visual or auditory cues. These findings contribute to the development of non-invasive sensory substitution in prostheses.

INDEX TERMS Proprioception, upper extremity amputation, tactile feedback, real-time feedback, neuromuscular electrical stimulation (NMES), human-in-the-closed-loop, myotome.

I. INTRODUCTION

The loss of upper limb function due to amputations creates both physical and psychological challenges for those affected [1]. Commercial prostheses have been developed to address motor performance needs. However, they fail to replicate the vital senses of tactile feedback and proprioception, which are essential for limb embodiment. As the largest human organ [2], the skin can somatotopically sense external stimuli, such as tactile sensation, through primary afferent neurons linked to mechanoreceptors. These sensory signals are transmitted to the thalamus for pre-processing,

The associate editor coordinating the review of this manuscript and approving it for publication was Woorham Bae.

then to the cerebral cortex, and finally, organized into a somatotopic map by the primary somatosensory cortex [3]. Without these senses, daily tasks can become difficult for amputees, as tactile feedback provides information about objects in contact with the skin, and proprioception provides body movement awareness.

To address this challenge, researchers have explored the feasibility of providing prosthesis users with sensory information via invasive and non-invasive methods such as mechanotactile, vibrotactile, temperature feedback, auditory feedback, and electrical stimulation (ES) [4]. However, ES is generally favoured due to its ease of use, lightweight nature, and adjustable parameters for stimulating nerve fibres in the skin and underlying tissues. It is classified into neuromuscular electrical stimulation (NMES) [5], functional electrical stimulation (FES) [6], and transcutaneous electrical nerve stimulation (TENS) [7]. FES and NMES are similar in their operation during muscle treatment [8]; compared with TENS units, which provide pain relief, NMES emits stronger and broader electrical pulses [9]. Generally, ES is applied on the neck [10], arm [11], wrist [12], tongue [13], and phantom digits [14] for the transmission of sensory information.

Zhang et al. proposed electrical stimulation via biphasic pulse alternating current (AC) with parameters of 7mA, 50Hz, and 600μs. They applied this stimulation for 12 hours to stimulate phantom limb digits and reproduce the tactile sensation. Even though they reported that participants successfully recognized three different sizes of grasped objects during their trials, their experiment was conducted on only one trans−radial amputee, and proprioception was not considered in their investigation [15]. Abbass et al. also elicited tactile feedback via electrical stimulation in the mode of current-controlled, charge-balanced biphasic pulses with a current amplitude of 0−10mA, frequency of 1 to 400Hz, and pulse width of 50 to 500μs. They used a custom-made multi-point electronic skin with matrix electrodes for spatial and patterned electrical stimulation on the forearm [16]. However, since their study did not include prostheses, valuable data on how their work can affect or benefit amputees was missed.

Additionally, Gu et al. presented simultaneous tactile feedback through ES for soft hand prostheses. In this closed−loop control system, the trigger to generate an electrical pulse had stable pulse variables with an amplitude of 4mA, a pulse width of 200μs, and a pulse frequency of 20Hz to stimulate phantom limb digits [17]. In this investigation, using pattern recognition, surface electromyography (sEMG) signal features were classified into four gestures to control the hand prosthesis. However, no control modulation method was used to adjust the electrical pulse variable.

Although the ES is a non−invasive approach for electrical impulses, it is characterized by interference in sEMG signals, resulting in reduced accuracy and prosthesis control due to frequency interference [18]. Additionally, this method does not allow users to perceive accurate movements because it is not well modulated for activating deep muscles, which are crucial to unlocking proprioception [19].

An alternative to ES sensory feedback for prostheses can be NMES. The NMES impulses are similar to impulses naturally produced by the nervous system and injected by electrodes placed on the skin near the target muscles. In this approach, the electrodes' polarity switching modes can be configured in monopolar and bipolar [20].

To have rich sensory-motor information (*i.e.*, motor control with sensory feedback), electrical stimulation could be evoked in afferent and efferent nerves [21]. To this end, this paper proposes neuromuscular electrical stimulation, which involves the application of electrical impulses to a group of muscles (myotomes) and peripheral nerves. By this approach, we aimed to overcome the challenges of non-invasive ES to stimulate deep muscles and non-somatotopically reproduce proprioception and tactile sensation by using the NMES controlled and regulated intensity by the hybrid proportional-differential (PD)-Fuzzy, which was operated by our custom-made myoelectric prosthetic hand to reach a sophisticated prosthesis.

As a result, our proposed approach allows the user to distinguish three different levels of force and stiffness intuitively. In summary, the contributions of this paper are as follows. Firstly, we studied myotomes as new stimulation sites to distinguish sensory feedback. Secondly, the closed-loop control system extends the human-in-the-closed-loop approach, giving real-time force and position feedback in conjunction with the users' tactile and proprioception awareness. Amputees and non-disabled participants experienced sensory stimulation on their myotomes to control prosthesis with EMG signals. This improved the prostheses' manipulation accuracy, reliability, and embodiment through sensory feedback and recall of proprioception and tactile feedback.

The rest of this paper is organized as follows: Section II describes our method and system overview. Then, in Section III, we present the experiments conducted and the results in detail, and the discussion and conclusions are given in Sections IV and V.

II. METHODS AND MATERIALS

A. STUDY DESIGN

In order to study whether the sensory information reproduced can be utilized by users in a closed-loop control system synchronized with an artificial limb, we employed C6 and C7 myotomes located near the elbow joint (outside and inside, without functionally overlapping). The C7 myotome region was stimulated to retrieve the tactile feedback, and C6 was elicited to recall proprioception information. In this case-control investigation, the trials were planned to evaluate the capability of participants to balance the grasping force and the angle of closure of the index finger of a bionic hand according to the outputs of a hybrid PD-Fuzzy controller to determine the size and physical properties of objects. The production of

TABLE 1. Participant characteristics.

Healthy			Amputee					
Sub.	Age (Year)	Gender	Sub.	Age	Gender (Year)	Amputation location	Time Elapsed (Year)	Prosthesis usage
H1	26	F	A1	37	M	Wrist disarticulation	37	Myoelectric
H2	24	F	A2	39	M	Short below elbow	41	Abandonment
H3	25	M	A3	42	M	Very short below elbow	47	Body-powered
H4	26	M	A4	45	M	Very short below elbow	50	Myoelectric
H5	19	M	A5	47	M	Long below elbow	48	Abandonment

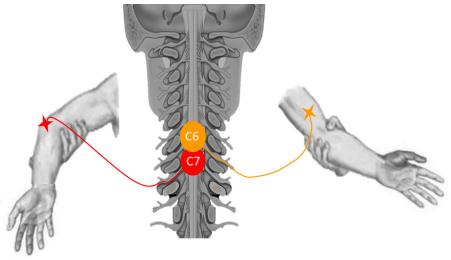

FIGURE 1. The C6 myotome is located at the cubital fossa's tendon of the biceps brachii muscle. The C6 controls elbow flexion, and it is innervated by the thumb by the median nerve branches. The C7 myotome is located at the tendon of the triceps brachii muscle, posterior to the elbow. The C7 controls the elbow extension, which is rooted to the arm's back and into the middle finger.

data modulation resulting from the controller system, directly and indirectly, affected the intensity of NMES based on recorded data from the force resistance sensor (FSR), a flex sensor, and the generated sEMG signal by the user.

The experiments took place for six weeks, with each session being about 60 minutes long and occurring once a day every week for each person involved.

B. SUBJECT RECRUITMENT

Five non-disabled as the control group (three males and two females, 24±2.91 years old) and five amputees (five males, 42±4.12 years old) were involved in the experiments (Table 1). All participants were informed about the study's potential benefits and risks before signing a written informed consent form for participation. The experimental protocols complied with the Declaration of Helsinki. Subjects with amputated limbs had normal sensory-motor function. None of them had other neurological, muscle tissue loss, psychiatric, or medical problems apart from those listed in Table 1. Also, the participants had not experienced NMES before the trials. This study received ethical approval from the Institutional Review Board of Tsinghua University under registration number 20210136.

C. BIDIRECTIONAL PROSTHESIS WITH REAL-TIME HYBRID CONTROL

A general review of the closed-loop system controlled by the hybrid PD-Fuzzy configuration is illustrated in Figure. 2. Our proposed multimodal sensory feedback system for closed-loop control of a prosthetic hand contains five modules: A) signal acquisition, B) signal processing, C) signal conversion, D) myotome stimulation, and E) biofeedback control.

The varied amplitude of the voltage of the sensory stimulation was modulated based on the force, position, and intensity of the sEMG signal (which is fed back into the control system). We exploited the bidirectional prosthesis layout based on a combination of custom-made hardware and software code to realize the proposed method. We installed the sensory closed-loop system on our customized prosthetic hand with seven degrees of freedom (DOFs) controlled by the sEMG signal.

The hardware created (Figure 3) was made up of an STM32F103C9T6 microcontroller (from ST Microelectronics in the US) with a 72MHz speed and 12-bit ADC ports. The hybrid PD-fuzzy controller was written on the microcontroller using the Arduino IDE platform. Figure 4 demonstrates the flowchart of the software design.

In this investigation, two pairs of flexible self-adhesive electrodes (cathode and anode, 40 × 20mm) were proposed to meet the comfort needs of daily routine activities. The low number of electrodes could reduce the possibility of desensitization and spatial interference. Also, the muscular response elicited by electricity may cause a decrease in muscular activity and shift the power spectrum to a higher frequency, leading to a decreased amplitude of the sEMG signal [22]. On the other hand, the frequency of electrical stimulation plays a crucial role in impacting sEMG signal discrimination. An inappropriate or inconsistent frequency may cause frequency interference from the electrical stimulation artefact [23], [24], leading to low accuracy in sEMG signal identification. Thus, the "elbow-flexion" (C6) and "elbow-extension" (C7) [25], [26] myotomes were selected to stimulate specific efferent and afferent nerves due to being innervated by distinct spinal nerves [25], avoid muscles overlapping, and have a high density of mechanoreceptors [27], Figure 1.

Self-adhesive electrodes were placed near sEMG sensors with low numbers to prevent desensitization and interference. A sinusoidal pulse current with an amplitude from 0 to 60mA and a constant frequency of 2Hz was used for stimulation to enhance reliability and prevent interference with sEMG signals' frequency domain. The polar shifting of electrodes was adjusted in monopolar mode to avoid electrode polarity changes and evade stimulating other myotomes.

Furthermore, we separated the myoelectric control system's electrical sources (batteries) and the main control board

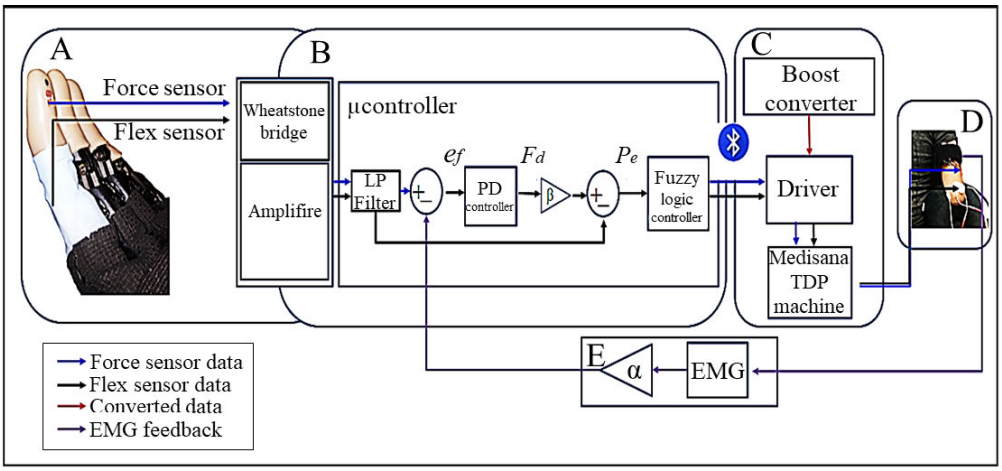

FIGURE 2. Flowchart of force and position sensory feedback by NMES on myotomes: (A) Signal acquisition. (B) Signal processing. (C) Signal conversion. (D) Myotome stimulation. (E) Biofeedback control.

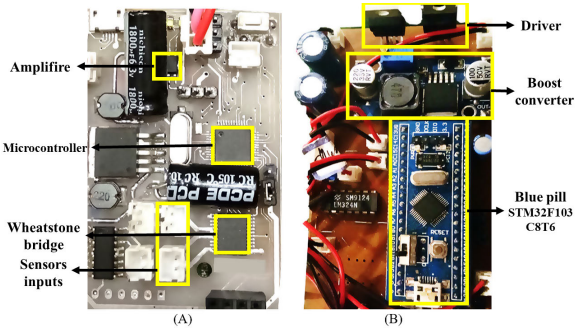

FIGURE 3. The developed hardware: (A) Main control board (B) Driver of NMES generator machine.

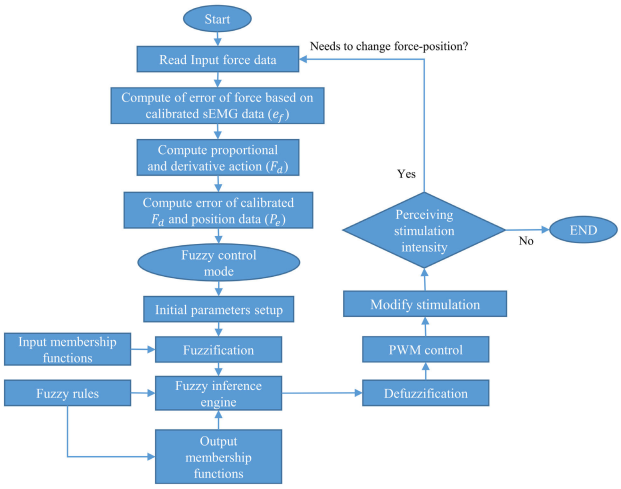

FIGURE 4. Flowchart of the software design.

to prevent electrical stimulation interference. The ''Myotome Stimulation'' segment and ''Biofeedback Control'' also had different electrical sources. The data received from the ''Signal Processing'' module was transmitted wirelessly to the ''Signal Conversion'' module to protect the main electronic board from the electrical stimulation artefacts. By performing these setups, the participants could control the bionic hand using arm muscles while simultaneously receiving relevant tactile and proprioceptive information employing NMES operated on myotomes.

Although we attempted to eliminate the electrical stimulation interference generated by NMES onto sEMG signals (to provide high-resolution sensory feedback with a comfortable feeling), this study did not quantify the impact of isolation on the electrical stimulation artefacts and frequency interference, as these were beyond the scope of this study.

a: SIGNAL ACQUISITION

In the signal acquisition of embedded sensors, a force-sensing resistor (FSR) sensor (*Taidacent*, China, 20g-2kg) and a flex sensor (SEN10264, *Sparkfun*, United States) were mounted on the prosthetic hand's index digit. A Wheatstone bridge was used to measure the small changes in the resistance of the sensors. Then the INA128 amplified the data to improve the measurement accuracy. Finally, the applied force ranged from 50 to 550g of gravitational force, and the joint angle was from 0°-110°. With muscle contraction, the sEMG signal was acquired from the biceps muscle by an sEMG electrode (13E200, *OttoBock*, Germany). The sampling rate frequency of the sEMG electrode was 1kHz. The raw sEMG signal was sequentially filtered by an infinite impulse response fourth-order Butterworth filter between 15 and 375Hz, and a notch filter removed noise at 50Hz.

b: SIGNAL PROCESSING

The data from the ''Signal Acquisition'' segment is filtered by a low-pass filter in the ''Signal Processing'' section and then transmitted to the hybrid PD-fuzzy controller. The modulated data was wirelessly transmitted to the ''Signal Conversion'' module.

In ''Signal Conversion,'' an external driver adjusted the voltage amplitude of the machine's stimulation power according to received data, which consists of sensory information

about the joint angle and the applied force based on the sEMG signal state gathered from the signal processing module.

In the "Myotome Stimulation" module, two channels of the NMES generator machine (*Medisana*, Germany) excite the myotomes with self-adhesive electrodes. The hybrid PD-Fuzzy controls the driver based on sEMG, force, and position feedback. The controller consists of two sections: inner and outer control loops. The outer loop controls the force. The inner loop controls the outer loop (force) and optimal position. PD controllers consist of two parallel types: derivative controllers and integral controllers. The derivative controller follows changes caused by proportional action and adapts to changes in the input based on the difference between the calibrated sEMG amplitude and the input force (e_f). The inner control loop, the fuzzy logic controller, was then used to improve the anti-interference performance and tune the system parameters used by the position error fuzzy controller input. In the outer control loop, the relationship between the applied force (F_i) and resistance variation can be expressed as [28]:

$$F_i = \left(\frac{1}{((\frac{V_s}{V_G}) - 1)mR_L}\right) - \frac{n}{m} \tag{1}$$

The relation between the constants m and n can be revealed by curve fitting. R_L is the resistance from the FSR sensor to the Wheatstone bridge, and V_s/V_G is the resistance variation, where V_s and V_G are the input and output voltages of the Wheatstone bridge, respectively. The input error (e_f) of the PD controller is the FSR sensor output subtracted by the voltage of the sEMG signal multiplied by a ratio coefficient α, which can be calibrated for each participant. Through the calibration, the PD-fuzzy controller applies the optimal stimulation intensity (F_d) of the applied force between the tip of the index finger and a grasped object:

$$F_d = K_{fp}e_f + K_{fd}\dot{e_f} \tag{2}$$

where K_{fp} and K_{fd} are the proportional and differential coefficients, the relationships between the resistance variations R(ϕ) and the bending angle ϕ of the flex sensor can be expressed as [29]:

$$R^0 = R^0_{sheet}\frac{L}{W} \tag{3}$$

where L is the length and R^0_{sheet} is the constant sheet resistance. Therefore, in practical testing, $D(\phi)$ is calculated based on the values of R(ϕ), R^0, and W. Then, for further simplification, $D(\phi) = \phi * \tau$ is considered, where τ is a constant variable obtained from experiments. As a result, ϕ with a range of 0°-110° is used as the input of the fuzzy controller, with the error of the position (P_e) expressed as:

$$P_e = \beta F_d - D(\phi) \tag{4}$$

In this paper, the PD controller adjusts the optimal force of the index finger. The coefficients α and β were in the range of practice tests based on each participant. In an early stage, after adjustment by the PD controller, the position error is the input

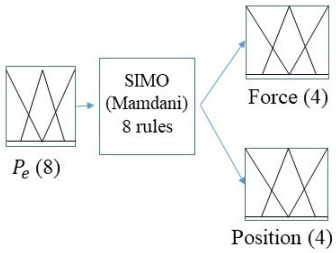

FIGURE 5. Single-input and multiple-output fuzzy logic units.

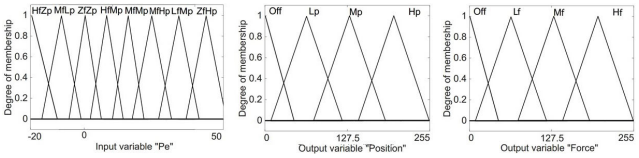

FIGURE 6. Triangular membership functions selected for input and output.

TABLE 2. Rules of the FLC.

1. If (P_e is HfZp) then (Position is Off)(Force is Hf) (1)
2. If (P_e is ZfHp) then (Position is Hp)(Force is Off) (1)
3. If (P_e is HfMp) then (Position is Mp)(Force is Hf) (1)
4. If (P_e is MfMp) then (Position is Mp)(Force is Mf) (1)
5. If (P_e is MfLp) then (Position is Lp)(Force is Mf) (1)
6. If (P_e is ZfZp) then (Position is Off)(Force is Off) (1)
7. If (P_e is LfMp) then (Position is Mp)(Force is Lf) (1)
8. If (P_e is MfHp) then (Position is Hp)(Force is Mf) (1)

of Mamdani's fuzzy inference system [30]. The fuzzy logic unit (FLU) is a single-input, multiple-output (SIMO) system with input (P_e) in the range of (-20 to 50) from practical tests and eight triangular membership functions (MFs). Moreover, the FLU has two outputs (within the range of 0 to 255) with four triangular membership functions (MFs). The FLU outputs were named force and position.

Three parameters affect the input of the FLU (P_e). To control the stimulation intensity on myotomes, two output parameters (the force and position) from the FLU were extracted as pulse width modulation (PWM) signals between 0 and 255, which were directly imported to the driver (as controlling signals) of the Medisana TDP machine. The input of the FLU (P_e) was clustered into eight segments: high-force and zero-position (HfZp), medium-force and low-position (MfLp), zero-force and zero-position (ZfZp), high-force and medium-position (HfMp), medium-force and medium-position (MfMp), medium-force and high-position (MfHp), low-force and medium-position (LfMp), and zero-force and high-position (ZfHp). Moreover, every output (position or force) of the FLU was clustered into four segments: (Off), low position (LP), medium position (MP), and high position (HP) for the position; and (Off), low force (LF), medium force (MF), and high force (HF) for the force. The FLU membership functions and rules are demonstrated in Figure 6, and Table 2 and Table 3, respectively. Additionally, the surface plot of the designed rules is depicted in Figure 7.

TABLE 3. Input and outputs ranges defined for FLU.

Input(P_e)	
Membership function	Range
MF1='H_F_Z_P'	[-20 -20 11]
MF2='H_F_H_P'	[47 50 50]
MF3='H_F_M_P'	[1 6 11]
MF4='M_F_M_P'	[11 17 23]
MF5='M_F_L_P'	[-11 -6 -1]
MF6='Z_F_Z_P'	[-1 0 1]
MF7='L_F_M_P'	[23 29 35]
MF8='M_F_H_P'	[35 41 47]
Output (Force)	
Membership function	Range
MF1='L_F'	[5 45 85]
MF2='M_F'	[85 127.5 170]
MF3='H_F'	[170 255 255]
MF4='Off'	[0 0 5]
Output (Position)	
Membership function	Range
MF1='L_P'	[5 45 85]
MF2='M_P'	[85 127.5 170]
MF3='H_P'	[170 255 255]
MF4='Off'	[0 0 5]

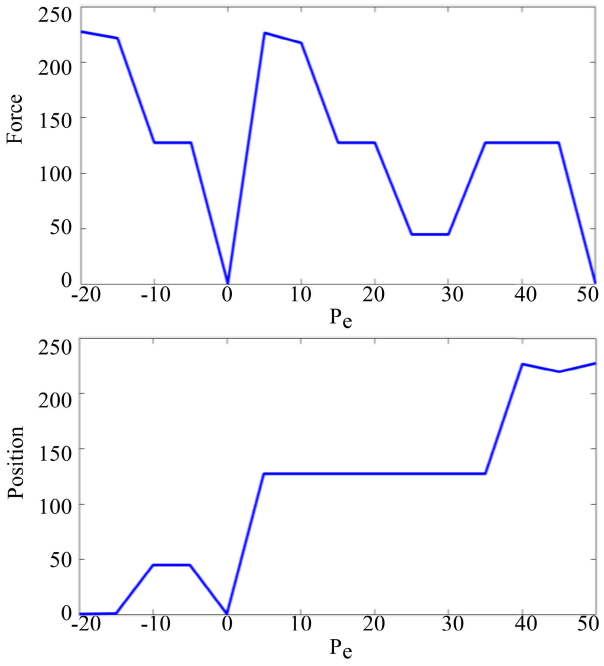

FIGURE 7. The surface plot of the designed rules.

c: SIGNAL CONVERSION, MYOTOME STIMULATION, AND BIOFEEDBACK CONTROL

In the "Signal Conversion" section, the output data from the FLU was transmitted wirelessly by the AT-09 Bluetooth 4.0 BLE Module (*HiLetgo*, China) to the driver of the Medisana TDP machine to determine the stimulation intensity in the form of PWM signals. Moreover, a DC-DC booster (MSDU20-XL6009, China) with a separate electric source was used as the voltage supplier and driver of the Medisana TDP machine due to its limited output voltage and the need to isolate other electronic circuits from electrical stimulation artefacts interference.

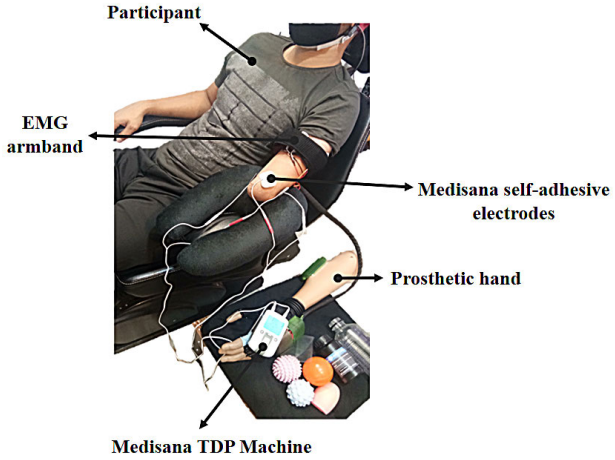

FIGURE 8. (a) The examiner stimulated myotomes. (b) Sensory feedback with noninvasive stimulation of myotomes with the help of the Medisana TDP machine (Medisana, Germany).

In the "Myotome Stimulation" module, the stimulation of myotomes with low-frequency monophasic sinusoidal pulses was exploited at 2Hz.

In this paper, the sEMG signal had two controlling functions: opening and closing the prosthesis and defining the fingers' motion velocity; in this regard, motion velocity was modulated based on the voltage amplitude of the received sEMG signal. Another function was a biofeedback role for the hybrid PD-fuzzy controller. The recorded voltage of the sEMG signal is passed through a proportional controller with a calibrated gain factor α, which the user generates in the "Biofeedback Control" module by contracting the muscle (Biceps) to open or close the prosthetic hand's digits based on the perceived intensity of stimulation on the myotomes.

D. STATISTICS AND DATA ANALYSIS

All data were analyzed using SPSS (Statistical Program for Social Sciences, version 22). We used the mean, standard deviation (SD), and percentage for descriptive statistics. In addition, the quantitative variables were expressed as mean SD, and the qualitative variables in numbers and percentages. All randomization for the experiment was accomplished with the random number generator in MATLAB (2020b version). Furthermore, the data's normality was initially tested with the Kolmogorov-Smirnov test when it was recorded. The unpaired two-sample t-test with a 95% confidence interval was performed to compare the means of the significantly independent groups (control and amputee) in the experiments.

III. EXPERIMENTS AND RESULTS

A. EXPERIMENTAL DESIGN

Five amputees and five non-disabled participants sat separately on a chair during experiments while isolated from their auditory and visual feedback. Amputee participants

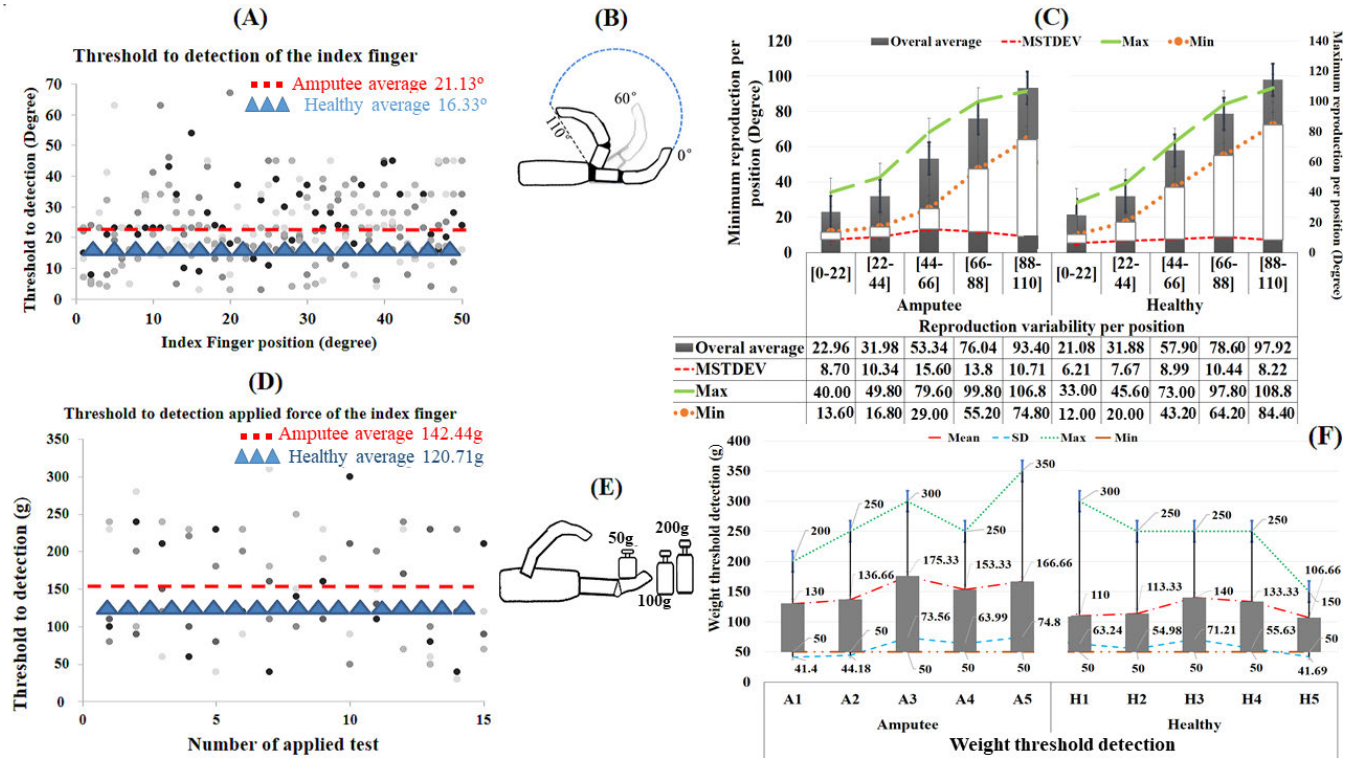

FIGURE 9. (A) The overall average detection threshold for changes in the prosthesis finger's angular movement obtained from the amputee participants was 21.13° and that of the non-disabled was 16.33°. (B) The complete range of the [0°-110°]. (C) Reproduction variability per position. (D) The detection threshold for the applied force of the index finger in healthy and amputee participants. (E) An example of recalling the applied force based on the perception of sensory stimulation by the entered gravitational force. (F) Details of the sensed threshold of the applied force.

symbolically used the prosthesis socket due to their remaining muscles' different sizes and lengths, as shown in Figure 8.

Although they had not received lengthy and regular training, they understood how to manipulate the bidirectional prosthesis. Five experiments were conducted. The detection of threshold in active motion and force ($n = 50$ and $n = 15$, repetitions of the experiment, respectively), joint angle reproduction, weight recognition, size, and stiffness identification ($n = 25$). The following sections will explain how these trials were conducted.

a: PRE-EXPERIMENTS PREPARATION

Before the experiments, all control structures and parameters, such as adjusting the hybrid control system, the electrode location, and stimulation intensity, were calibrated based on the participant's comfort level. A clinical expert identified the optimal distance between the anode and cathode to prevent skin irritation. Because a shortened distance results in a tingling sensation at both the cathode and anode, and a long distance prevents users from feeling sensory impulses [30]. Moreover, an optimal distance between the sensory mediator electrodes and the sEMG sensor was tried to avoid electrical interference and prevent skin irritation. Each participant experienced the initial preparations separately to verify the effects of sensory stimulation on the amputee's ability to embody the prosthesis. Also, if sensory impulses on this part of the myotome were inconvenient, another area of the myotome was employed as an alternative site.

Training sessions to demonstrate active prosthesis control through an sEMG signal were held with short-term general training sessions (<15min). First, participants observed hand states (open and close) while grasping objects using auditory and visual feedback without NMES. Second, to ensure the perception of sensory input before the trials, the examiner passively put the prosthetic hand's digit into the desired angular intervals ((0°-22°), (22°-44°), (44°-66°), (66°-88°), and (88°- 110°)). Each participant was asked to observe the artificial hand's digit position and perceive the intensity changes of impulses in each angular interval.

Afterward, the participants were asked to demonstrate the artificial hand's digit positions on their healthy index finger (participant A5 was excluded due to the type of his amputation). Third, we tested if participants could feel simultaneous feedback from two sensory channels by asking them to hold objects of different properties and sizes and report any sensations. We repeated the calibration process three times per myotome. None of the participants reported a cross-talk sensation while simultaneously, myotomes C6 and C7 were stimulated. Finally, the Medisana TDP machine's stimulation power was calibrated using the average minimum and maximum intensities to adjust α and β.

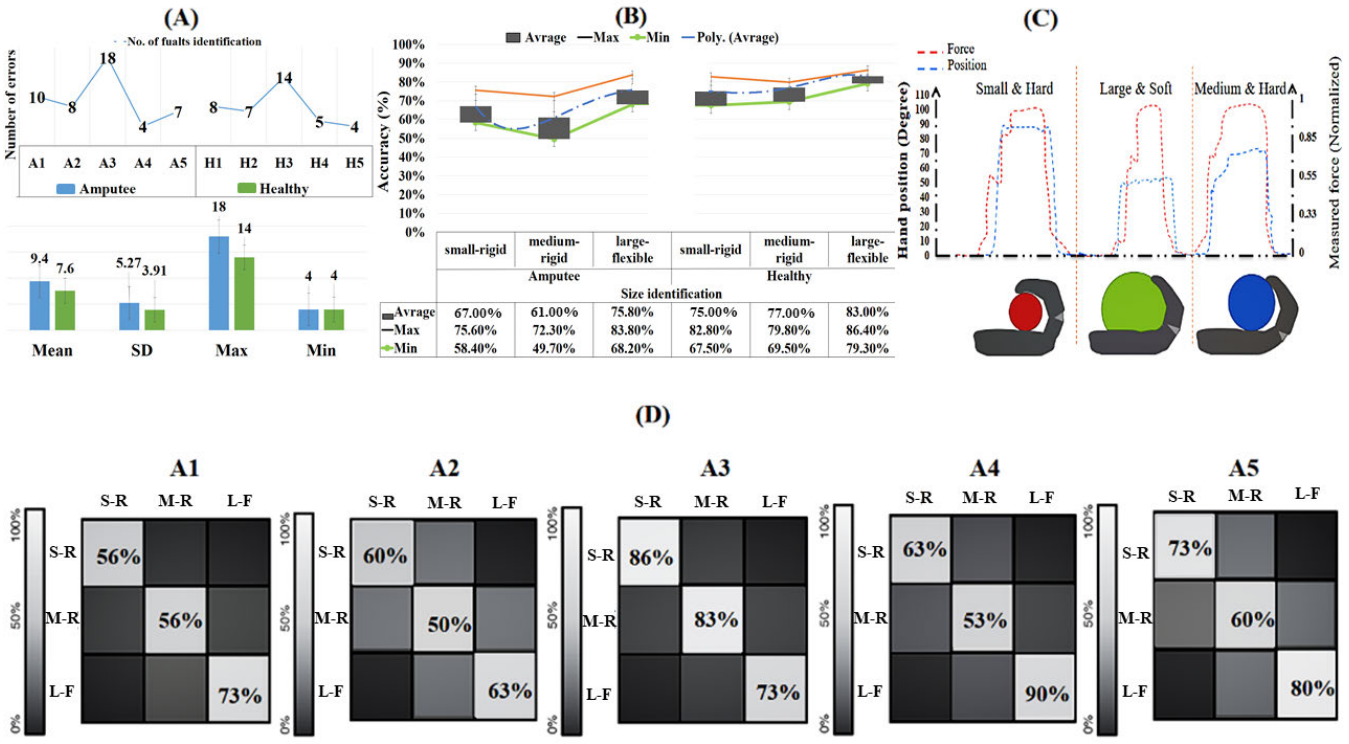

FIGURE 10. (A) The number of errors before the participants provided the desired answers and more details for the comparison of amputee and healthy performance. (B) The overall average number of correct responses and variations within a data set of healthy and amputee participants in 25 repeated trials. (C) The overall performance with both inputs and remapped proprioception in different objects. (D) The overall performance of the amputee participants for remapped proprioception (S-R = "small-rigid," M-R = "medium-rigid," and L-F = "large-flexible").

b: DETECTION OF THRESHOLD IN ACTIVE MOTION AND FORCE

Five individuals with amputations and five non-disabled ones participated in experiments to find their sensory thresholds (the lowest amount of stimulation a participant can sense) by actively controlling the prosthesis. To calibrate the intensity of the sensory stimulation, two levels were selected: ''low-level'' and ''high-level.'' The ''low-level'' was the minimum amount of power with which participants could perceive sensory impulses. Meanwhile, the ''high-level'' was the maximum intensity that made every participant uncomfortable. Myotomes C6 and C7 were stimulated separately in the proprioception and tactile threshold experiments. In the proprioception threshold experiment, the participants were asked to change the index digit of the prosthesis voluntarily by their own sEMG signal from 0° (without the intensity of stimulation, fully opened) to 110° (maximum intensity of stimulation, fully closed) and vice versa, from 110° to 0°. The participants reported that as soon as stimulation (C6 myotome) was sensed or cut off, then the examiner recorded the angular position according to the angle monitored by the prosthesis. The experiment was repeated 50 times at a constant speed of approximately 7°/s for each participant (Figure 9(A)(B)). In another experiment, the examiner measured participants' sense of touch thresholds by putting different standard weights (*ZunateFditCalibrationWeight*, Germany) on the index finger. The participants reported impulses on the C7 myotome as soon as they were perceived. This experiment was repeated 15 times (Figure 9(D)(E)(F)).

c: JOINT ANGLE REPRODUCTION

We designed this experiment to reproduce the prosthetic hand's digit's angular motion to determine the proprioception quality of amputee participants. In this trial, the healthy and amputee participants were instructed to position the index finger of the prosthesis into the five angular intervals by perceiving stimulation on myotome C6 with self-generated EMG. Participants actively moved the index finger from 0° with a constant speed of approximately 7°/s to the five desired angular intervals within the range of 0° to 110°. This trial was repeated until the finger had been located in the desired angular interval, see Figure 9(C).

d: WEIGHT RECOGNITION

We evaluated the accuracy of tactile feedback by having participants determine the weight on the index finger of the prosthetic hand and report relative weight levels (light, moderate, and heavy) based on stimulation intensity on the C7 myotome. Using only three standard weights (50g, 100g, and 200g) placed on the FSR sensor, we repeated the above exercise until the participants could correctly distinguish the weights (Figure 10(A)). The steps involved creating a list of

the three weight options and randomly mixing them up. Each participant was then given a weight in the order of the list.

e: SIZE AND STIFFNESS IDENTIFICATION

This experiment aimed to simulate daily routine activities by integrating proprioception and tactile feedback while grasping objects with the prosthetic hand. The trial involved non-disabled and amputee participants identifying the size and stiffness of objects. Participants were asked to report the type of grasped objects with 25 repetitions of the test. Three cylindrical bottles with different diameters (3cm, 4.5cm, and 5.46cm) and material types (flexible and rigid) were employed; they were designated as ''small-rigid,'' ''medium-rigid,'' and ''large-flexible'' cylinders, respectively, as shown in Figure 10(B)(C)(D). Participants randomly grabbed the objects with active control of the prosthesis based on the protocol described earlier.

B. RESULTS

a: DETECTION OF THRESHOLD IN ACTIVE MOTION AND FORCE

In the proprioception thresholds experiment, the overall average sensory threshold for amputee participants was 21.13° in the whole range of (0°- 110°); for non-disabled participants, it was 16.33°, as shown in Figure 9(A). Moreover, in the sense of touch thresholds experiment, as shown in Figure 9(E), the results showed that the mean and standard deviation (M±SD) of the sensory thresholds for amputee participants A1 to A5 were 152g±76.61, 166g±73.85, 154g±60.33, 44g±78.81, and 146g±89.90, respectively, Figure 9(F). The overall average sensory threshold for healthy and amputee individuals was 120.7g and 152.4g, as shown in Figure 9(D). The unpaired two-sample t-test observed in the detection of threshold in force had a statistically significant difference in mean between the two groups ($T(8) = 2.91$, P-value $= 0.007$).

b: JOINT ANGLE REPRODUCTION

Amputees and non-disabled participants tested joint angle control on the prosthetic index finger by changing stimulation intensity proportional to angular position. Results showed no difference in sensory threshold in the opening/closing direction. However, accuracy was limited in identifying angular positions between 0-22° due to overlap with the mean 21° sensory threshold. Only one amputee and one non-disabled participant could control the index finger at this range. Leading to the means and standard deviations (M±SD) recorded by amputee participants were in the ranges of 22.96°±8.70, 31.98°±10.34, 53.34°±15.60, 76°±13.80 and 93.40°±10.71. Likewise, non-disabled participants reported 21.08°±6.21, 31.88°±7.67, 57.90°±8.99, 78.60°±10.44 and 97.92°±8.22, as shown in Figure 9(C). The unpaired two-sample t-test observed only in one angular interval, [88°-110°], the statistically significant difference in mean between the two groups ($T(98) = 2.36$, P-value $= 0.03$).

c: WEIGHT RECOGNITION

The minimum and maximum numbers of false predictions were as follows: The best performance was reported for A4 (amputee participant) and H5 (healthy participant) with four errors, and eighteen errors for A3 (amputee participant) were recorded as the worst performance, as shown in Figure 10(A). The unpaired two-sample t-test showed no statistically significant difference in the mean of faults of weight predictions between the two groups ($T(8) = 0.61$, P-value $= 0.53$).

d: SIZE AND STIFFNESS RECOGNITION

Grasped bottles with different sizes and stiffness evoked different angular positions and forces on the index finger in the embedded sensors of the prosthetic hand, allowing users to identify objects' size and hardness according to sensory information fed back on their myotomes. Figure 10(B)(C) shows the state of the objects grasped by the prosthetic hand and the overall average number of correctly reported results by the amputee and non-disabled participants in 25 repetitions. Amputee participants' overall average accuracy was 68%; the accuracy was recorded at 67% for ''small-rigid,'' 61% for ''medium-rigid,'' and 76% for ''large-flexible'' cylinders. In addition, the overall performance of integrating proprioception and tactile feedback for the amputee participants was reported as a confusion matrix, in which participant A3 recorded the best average performance at 80.66%, as shown in Figure 10(D). Also, non-disabled participants' overall average accuracy was 78.3%, and reported as 75% for ''small-rigid,'' 77% for ''medium-rigid,'' and 83% for ''large-flexible,'' as shown in Figure 10(B), with no statistical difference accuracy between the two groups ($t(4) = 2.07$; P-value $= 0.07$).

IV. DISCUSSION

This study showed that NMES, regulated by the hybrid PD-fuzzy controller, allows amputees to control their prostheses in real-time and simulate proprioception and tactile feedback while grasping objects. The performance of the closed-loop system was evaluated through dexterous manipulation simulations of daily tasks. The hybrid PD-fuzzy controller adjusted stimulation intensity based on feedback from the force, position, and sEMG signal. Both amputees and non-amputees (control group) felt changes in the stimulation intensity on their muscles, demonstrating efficient and synchronized delivery of proprioception and tactile information. Participants could sense small changes in stimulation intensity during movement, force, weight, and joint angle tests, although results varied for individual participants.

The trial of ''joint angle reproduction'' illustrated that the participants could achieve well-defined perception caused by sensory substitution through the closed-loop control system in the bidirectional prosthetic hand. In healthy fingers, the sensory threshold had been reported between 1.5° and 6.5° [35], while with the invasive method in amputee

TABLE 4. Comparison between investigations on non-invasive sensory feedback using ES.

Ref.	Sensor	St. area	St. channels	Sub.	Method	Freq. (Hz)	Current direct	Platform	Performance
[10]	1 FSR 2 Flex	Neck	2	8 Healthy	Current amplitude modulated	200	Mono-phasic	Healthy hand+ glove	Grip force and hand aperture correct identification (49.2%)
[12]	-	Wrist	2	10 Healthy	Channel-hopping interleaved pulse scheduling (CHIPS)	30	Biphasic	Healthy hand	Not measurements given
[31]	-	Forearm	2	13 Healthy	Pulse width,frequency encoding	70	Biphasic	Joy stick	Encoding of feedback frequency modulation: 83.4±4.1%
[32]	-	Forearm	24	8 Healthy	Spatial and frequency modulated coding	50	Biphasic	-	Success rate $>$ 90% in localizing
[33]	2 EMG 2 FSR 2 Flex	Forearm	5	15 Healthy	Spatial and pulse width coding	40	-	Prosthesis	Correct identification rates(CIRs)(size: 87.5%,Softness:94%, grasping force:73.8%)
[34]	8 EMG	Dominant-forearm	16	10 Healthy	Data blanking	50	Biphasic	Natural hand	Visual(90$<$) Combine(90$<$) Tactile(78$<$)
This Paper	1 sEMG 1 FSR 1 Flex	Myotome	2	5 Amputee 5 Healthy	hybrid PD-Fuzzy control	2	Mono-phasic	Prosthesis	Amputees result: Ave. threshold for action motion: 21°, Ave. threshold for force: 1.524 N, identification of sizes Small (74%), Medium (70%), Large (76%)

individuals, the median of the joint angle was determined to be 9.1° [35]. Although in [35], a prosthetic hand with fingers having three links (knuckles) was utilized, we used the customized bionic hand with two knuckles in this research. Even though fingers with a three-link structure have more shape-adaptivity and are more accurate in locating desired angular positions than other designs, this limitation did not affect the functionality of our prosthetic hand. We noted, however, that in our proposed method, the joint angle did not fit accurately at the 0°-22° angular interval. In the ''size and stiffness identification'' trial, the participants recognized three different cylinders, indicating their ability to distinguish between two channels of sensory stimulation, of which the results were as follows: 67% (small-rigid cylinder), 61% (medium-rigid cylinder), and 76% (large-flexible cylinder) for amputees and non-disabled were 75% for small-rigid, 77% for medium-rigid, and 83% for large-flexible.

Compared to the invasive method that D' Anna et al. had proposed, their results (89% for the ''small-hard'' object, 62% for the ''large-soft'' object, and 73% for the ''large-hard'' object) show that NMES has a reasonable prospect of recalling sensory information.

These trials show that each sensory substitution channel primarily conveys information about a single aspect of an object with no statistically significant difference between amputees and non-disabled, such as stiffness or size. The improved performance achieved by using multiple sensory feedback channels suggests that the proposed method could increase the number of channels while retaining high performance.

Table 4 compares our method with others from the past five (5) years. Other methods lack the recruitment of amputees for testing and functional experiments, with stimulation mainly in the forearm or wrist. Most studies did not use a control strategy for conveying sensory information, but our study tries to address these limitations.

Our future research will be concentrated on increasing the number of fingers studied by using different myotomes, investigating other perceptions that could be elicited by this method, and finally integrating the presented sensory closed-loop method with further investigations [36], [37].

V. CONCLUSION

In conclusion, this study shows that using NMES as biofeedback for bidirectional prosthetic hands is an influential trend that allows both non-disabled and amputee participants to use a multisensory fusion approach to reproduce proprioception and tactile sensation. The results achieved in the detection of thresholds in motion (16.33° and 21.13°, respectively) and weight (120.7g and 152.4g, respectively), joint angle reproduction, and size-stiffness identification (78.3% and 68%, respectively) verify that the prosthesis users can instantaneously employ the two sensory information channels for dextrous manipulation. Furthermore, our study attempts to demonstrate a clinical method to reproduce the sensory-motor function of daily routine tasks. Ultimately, our motivation for conducting this study was to pave the way for sophisticated prosthetic limbs to provide richer non-invasive feedback.

APPENDIX A
HARDWARE SPECIFICATIONS

Components	Brand	Model	Country
Processor	STMicroelectronics	STM32F103C9T	USA
Electrode	Medisana	87100	Germany
Force sensor	Taidacent	Tdfsr400	China
Flex sensor	Sparkfun	SEN10264	USA
Amplifier	Texas instrument	INA128AP	USA
Wheatstone bridge	Analogue Device	AD7730BRZ	USA
EMG sensor	OttoBock	13E200	Germany
NMES generator	Medisana	Pain therapy TDP	Germany
Bluetooth module	HiLetgo	CC2541	China
Boost module	HiLetgo	XL6009	China

REFERENCES

[1] J. K. Bradway and E. A. Malone, "Psychological adaptation to amputation: An overview," *Orthotics Prosthetics*, vol. 38, no. 3, pp. 46–50, 1984.
[2] J. E. Lai-Cheong and J. A. McGrath, "Structure and function of skin, hair and nails," *Medicine*, vol. 41, no. 6, pp. 317–320, Jun. 2013.
[3] E. E. Hagberg, R. Ackerley, D. Lundqvist, J. Schneiderman, V. Jousmäki, and J. Wessberg, "Spatio-temporal profile of brain activity during gentle touch investigated with magnetoencephalography," *NeuroImage*, vol. 201, Nov. 2019, Art. no. 116024.
[4] B. Stephens-Fripp, G. Alici, and R. Mutlu, "A review of non-invasive sensory feedback methods for transradial prosthetic hands," *IEEE Access*, vol. 6, pp. 6878–6899, 2018.
[5] E. Galofaro, E. D'Antonio, N. Lotti, and L. Masia, "Rendering immersive haptic force feedback via neuromuscular electrical stimulation," *Sensors*, vol. 22, no. 14, p. 5069, Jul. 2022.
[6] T. Schauer, "Sensing motion and muscle activity for feedback control of functional electrical stimulation: Ten years of experience in Berlin," *Annu. Rev. Control*, vol. 44, pp. 355–374, Jan. 2017.
[7] K. Kita, Y. Otaka, K. Takeda, S. Sakata, J. Ushiba, K. Kondo, M. Liu, and R. Osu, "A pilot study of sensory feedback by transcutaneous electrical nerve stimulation to improve manipulation deficit caused by severe sensory loss after stroke," *J. Neuroeng. Rehabil.*, vol. 10, no. 1, pp. 1–16, Dec. 2013.
[8] C. S. Bickel, C. Yarar-Fisher, E. T. Mahoney, and K. K. McCully, "Neuromuscular electrical stimulation–induced resistance training after SCI: A review of the dudley protocol," *Topics Spinal Cord Injury Rehabil.*, vol. 21, no. 4, pp. 294–302, Nov. 2015.
[9] C. Yue, X. Zhang, Y. Zhu, Y. Jia, H. Wang, and Y. Liu, "Systematic review of three electrical stimulation techniques for rehabilitation after total knee arthroplasty," *J. Arthroplasty*, vol. 33, no. 7, pp. 2330–2337, Jul. 2018.
[10] T. J. Arakeri, B. A. Hasse, and A. J. Fuglevand, "Object discrimination using electrotactile feedback," *J. Neural Eng.*, vol. 15, no. 4, Aug. 2018, Art. no. 046007.
[11] L. Jabban, D. Zhang, and B. W. Metcalfe, "Interferential current stimulation for non-invasive somatotopic sensory feedback for upper-limb prosthesis: Simulation results using a computable human phantom," in *Proc. 10th Int. IEEE/EMBS Conf. Neural Eng. (NER)*, May 2021, pp. 765–768.
[12] A. E. Pena, J. J. Abbas, and R. Jung, "Channel-hopping during surface electrical neurostimulation elicits selective, comfortable, distally referred sensations," *J. Neural Eng.*, vol. 18, no. 5, Oct. 2021, Art. no. 055004.
[13] C. A. Lozano, K. A. Kaczmarek, and M. Santello, "Electrotactile stimulation on the tongue: Intensity perception, discrimination, and cross-modality estimation," *Somatosensory Motor Res.*, vol. 26, nos. 2–3, pp. 50–63, Jan. 2009.
[14] D. Zhang, H. Xu, P. B. Shull, J. Liu, and X. Zhu, "Somatotopical feedback versus non-somatotopical feedback for phantom digit sensation on amputees using electrotactile stimulation," *J. Neuroeng. Rehabil.*, vol. 12, no. 1, pp. 1–11, Dec. 2015.
[15] J. Zhang, C.-H. Chou, X. Wu, W. Pei, and N. Lan, "Non-invasive stable sensory feedback for closed-loop control of hand prosthesis," in *Proc. 44th Annu. Int. Conf. IEEE Eng. Med. Biol. Soc. (EMBC)*, Jul. 2022, pp. 2344–2347.
[16] Y. Abbass, M. Saleh, S. Dosen, and M. Valle, "Embedded electrotactile feedback system for hand prostheses using matrix electrode and electronic skin," *IEEE Trans. Biomed. Circuits Syst.*, vol. 15, no. 5, pp. 912–925, Oct. 2021.
[17] G. Gu, N. Zhang, H. Xu, S. Lin, Y. Yu, G. Chai, L. Ge, H. Yang, Q. Shao, X. Sheng, X. Zhu, and X. Zhao, "A soft neuroprosthetic hand providing simultaneous myoelectric control and tactile feedback," *Nature Biomed. Eng.*, vol. 7, pp. 1–10, Aug. 2021.
[18] L. Jiang, Q. Huang, J. Zhao, D. Yang, S. Fan, and H. Liu, "Noise cancellation for electrotactile sensory feedback of myoelectric forearm prostheses," in *Proc. IEEE Int. Conf. Inf. Autom. (ICIA)*, Jul. 2014, pp. 1066–1071.
[19] S. Shokur, A. Mazzoni, G. Schiavone, D. J. Weber, and S. Micera, "A modular strategy for next-generation upper-limb sensory-motor neuroprostheses," *Med*, vol. 2, no. 8, pp. 912–937, Aug. 2021.
[20] E. L. Nussbaum, P. Houghton, J. Anthony, S. Rennie, B. L. Shay, and A. M. Hoens, "Neuromuscular electrical stimulation for treatment of muscle impairment: Critical review and recommendations for clinical practice," *Physiotherapy Canada*, vol. 69, no. 5, pp. 1–76, Nov. 2017.
[21] T. S. Davis, H. A. C. Wark, D. T. Hutchinson, D. J. Warren, K. O'Neill, T. Scheinblum, G. A. Clark, R. A. Normann, and B. Greger, "Restoring motor control and sensory feedback in people with upper extremity amputations using arrays of 96 microelectrodes implanted in the median and ulnar nerves," *J. Neural Eng.*, vol. 13, no. 3, Jun. 2016, Art. no. 036001.
[22] L. Cao, Y. Wang, D. Hao, Y. Rong, L. Yang, S. Zhang, and D. Zheng, "Effects of force load, muscle fatigue, and magnetic stimulation on surface electromyography during side arm lateral raise task: A preliminary study with healthy subjects," *BioMed Res. Int.*, vol. 2017, pp. 1–9, Apr. 2017.
[23] M. B. I. Reaz, M. S. Hussain, and F. Mohd-Yasin, "Techniques of EMG signal analysis: Detection, processing, classification and applications," *Biol. Procedures*, vol. 8, no. 1, pp. 11–35, Dec. 2006.
[24] L. Mcmanus, G. De Vito, and M. M. Lowery, "Analysis and biophysics of surface EMG for physiotherapists and kinesiologists: Toward a common language with rehabilitation engineers," *Frontiers Neurol.*, vol. 11, Oct. 2020, Art. no. 576729.
[25] J. Filshie, W. Adrian, and M. Cummings, *Medical Acupuncture: A Western Scientific Approach*, 2nd ed. Amsterdam, The Netherlands: Elsevier, 2016, pp. 262–287.
[26] O. Zaidat, A. Lerner, and J. D. Miles, *The Little Black Book of Neurology*. Amsterdam, The Netherlands: Elsevier, 2019, pp. 316–400.
[27] R. Rupp, C. Schuld, F. Biering-Sørensen, K. Walden, G. Rodriguez, S. Kirshblum, R. Betz, S. P. Burns, W. Donovan, D. E. Graves, J. Guest, L. Jones, A. Krassioukov, M. J. Mulcahey, M. S. Read, and K. Tansey, "A taxonomy for consistent handling of conditions not related to the spinal cord injury (SCI) in the international standards for neurological classification of SCI (ISNCSCI)," *Spinal Cord*, vol. 60, no. 1, pp. 18–29, Jan. 2022.
[28] S. Kursun Bahadir, "Identification and modeling of sensing capability of force sensing resistor integrated to E-Textile structure," *IEEE Sensors J.*, vol. 18, no. 23, pp. 9770–9780, Dec. 2018.
[29] G. Saggio, A. Lagati, and G. Orengo, "Shaping resistive bend sensors to enhance readout linearity," *Int. Scholarly Res. Notices*, vol. 2012, pp. 1–7, Nov. 2012.
[30] E. Méndez, O. Castillo, J. Soria, P. Melin, and A. Sadollah, "Water cycle algorithm with fuzzy logic for dynamic adaptation of parameters," in *Proc. Mex. Int. Conf. Artif. Intell.* Cham, Switzerland: Springer, 2016, pp. 250–260.
[31] J. L. Dideriksen, I. U. Mercader, and S. Dosen, "Closed-loop control using electrotactile feedback encoded in frequency and pulse width," *IEEE Trans. Haptics*, vol. 13, no. 4, pp. 818–824, Oct. 2020.
[32] L. Seminara, H. Fares, M. Franceschi, M. Valle, M. Strbac, D. Farina, and S. Dosen, "Dual-parameter modulation improves stimulus localization in multichannel electrotactile stimulation," *IEEE Trans. Haptics*, vol. 13, no. 2, pp. 393–403, Apr. 2020.
[33] G. Chai, J. Briand, S. Su, X. Sheng, and X. Zhu, "Electrotactile feedback with spatial and mixed coding for object identification and closed-loop control of grasping force in myoelectric prostheses," in *Proc. 41st Annu. Int. Conf. IEEE Eng. Med. Biol. Soc. (EMBC)*, Jul. 2019, pp. 1805–1808.
[34] M. A. Garenfeld, N. Jorgovanovic, V. Ilic, M. Strbac, M. Isakovic, J. L. Dideriksen, and S. Dosen, "A compact system for simultaneous stimulation and recording for closed-loop myoelectric control," *J. Neuroeng. Rehabil.*, vol. 18, no. 1, pp. 1–17, Dec. 2021.

[35] E. D'Anna, G. Valle, A. Mazzoni, I. Strauss, F. Iberite, J. Patton, F. M. Petrini, S. Raspopovic, G. Granata, R. Di Iorio, M. Controzzi, C. Cipriani, T. Stieglitz, P. M. Rossini, and S. Micera, "A closed-loop hand prosthesis with simultaneous intraneural tactile and position feedback," *Sci. Robot.*, vol. 4, no. 27, Feb. 2019, Art. no. eaau8892.

[36] A. S. Asheghabadi, S. B. Moqadam, and J. Xu, "Multichannel finger pattern recognition using single-site mechanomyography," *IEEE Sensors J.*, vol. 21, no. 6, pp. 8184–8193, Mar. 2021.

[37] S. B. Moqadam, A. S. Asheghabadi, F. Norouzi, H. Jafarzadeh, A. Khosroabadi, A. Alagheband, G. Bangash, N. Morovatdar, and J. Xu, "Conceptual method of temperature sensation in bionic hand by extraordinary perceptual phenomenon," *J. Bionic Eng.*, vol. 18, no. 6, pp. 1344–1357, Nov. 2021.

SAEED BAHRAMI MOQADAM received the B.S. degree in electronic engineering from Azad University, in 2013, and the M.S. degree in mechatronic engineering from Hakim Sabzevari University, Sabzevar, Iran, in 2016. He is currently pursuing the Ph.D. degree in mechanical engineering with Tsinghua University, Beijing, China.

From 2015 to 2018, he voluntarily served as the Head of the Team with Ferdowsi University, Mashhad, Iran, where he is in charge of designing and producing the FUM bionic hands I and II. In 2020, he developed and manufactured the first non-invasive, bidirectional prosthetic hand in Iran. His research interests include developing new strategies for functional electrical stimulation and control, biomechatronics, human–robot interaction and control, neural networks and machine learning, biomedical signal processing, and biomimetic robotic systems.

Mr. Moqadam received the Best Conference Paper Award, in 2016 and 2022, and the All-Around Excellent International Student Award from the Mechanical Department, Tsinghua University, in 2021.

KNOLLIS DELLE was born in Takoradi, Ghana. He received the B.Sc. degree in biochemistry from the University for Development Studies, Ghana, in 2019. He is currently pursuing the M.Eng. degree in energy and power engineering (nuclear engineering and nuclear technology management) with Tsinghua University.

In addition to his academic pursuits, he is an Assistant Program Officer with the Ministry of Energy and Control, Ghana. He has interned with the Council for Scientific and Industrial Research, Ghana, and GHACEM, a cement manufacturing company in Ghana. His research interests include encompass power systems, clean energy technologies, artificial intelligence, and machine learning. He is an International Electrotechnical Commission Young Professional, an Emerging Public Leaders of Ghana Fellow, and a Young African Leadership Initiative Fellow. He is a Microsoft-Certified Data Scientist and the Deputy Managing Editor of the AfroScience Network, Ghana. He has received multiple accolades, including recognition from the Gansu Natural Energy Research Institute, for contributing to an article on the energy situation in Ghana.

URSUS SCHORLING was born in Hannover, Germany, in 1994. He received the B.S. and M.S. degrees in mechanical engineering from Leibniz University Hannover, in 2018 and 2022, respectively, with a focus on design and construction in robotics and measurement and control engineering.

AHMAD SALEH ASHEGHABADI received the B.S. and M.S. degrees in mechanical engineering from Azad Najaf Abad University, Esfahan, Iran, in 2010 and 2015, respectively. He is currently pursuing the Ph.D. degree in mechanical engineering with Tsinghua University, Beijing, China. From 2011 to 2014, he was with the Adolescent Research Club for Robotics. From 2014 to 2018, he was a Lecturer with the Mechanical Engineering Club. His research interests include mechatronics, neural networks, and biosignal processing.

FARZANEH NOROUZI received the M.D. degree from the Mashhad University of Medical Sciences, Mashhad, Iran, in 2017. From 2017 to 2021, she studied the cardiovascular disease specialty with the Mashhad University of Medical Sciences. Since 2021, she has been a Cardiologist with the M. E. J. Hospital, Khorasan Razavi, Iran. Her research interests include developing new strategies for functional electrical stimulation, acupuncture, artificial intelligence, biostatistics, and heart failure.

JING XU (Member, IEEE) received the B.E. degree in mechanical engineering from the Harbin Institute of Technology, Harbin, China, in 2003, and the Ph.D. degree in mechanical engineering from Tsinghua University, Beijing, China, in 2008. He was a Postdoctoral Researcher with the Department of Electrical and Computer Engineering, Michigan State University, East Lansing, MI, USA. He is currently an Associate Professor with the Department of Mechanical Engineering, Tsinghua University. His research interests include vision-guided manufacturing, image processing, and intelligent robotics.